Measuring the Magnetic Anisotropy of Metal-Metal Multiple Bonds: The Importance of Correcting for Ligand Effects.

R. Joseph Lastowski,[a] Konstantinos D. Vogiatzis,[b] and Gregory S. Girolami*,[a]

[a] School of Chemical Sciences, 600 S. Mathews Avenue, University of Illinois at Urbana-Champaign, Urbana, Illinois 61801, United States

[b] Department of Chemistry, University of Tennessee, Knoxville, Tennessee 37996, United States

Graphic for TOC

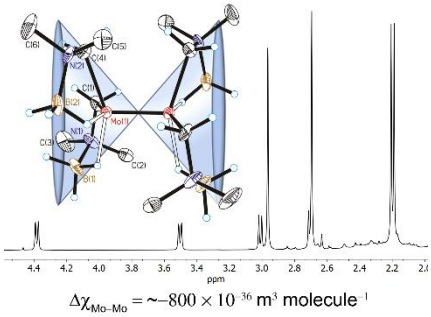

Synopsis

A method for correcting the magnetic anisotropies of metal-metal bonds (measured from structural and ^{1}H NMR data) for the effects of ancillary ligands is presented. Application of this method to the newly described molybdenum(II) dimer $Mo_2(CH_2NMe_2BH_3)_4$ suggests that the magnetic anisotropies of Mo–Mo quadruple bonds are much more similar to those of C–C triple bonds than previously estimated.

Abstract

We describe the synthesis and characterization of the quadruply-bonded dimer $Mo_2(CH_2NMe_2BH_3)_4$ in which each molybdenum(II) center is bound to two chelating boranato-dimethylaminomethyl (BDAM) ligands. The BDAM anions bind to the metal at one end by a

metal–carbon σ bond and at the other by a three-center M–H–B interaction. Each BDAM ligand chelates to a single Mo atom so that the metal-metal bond is unbridged; the Mo-Mo distance is 2.114(2) Å. Solid-state structural and solution NMR data, analyzed via McConnell's equation and supported by DFT calculations, show that the magnetic anisotropies associated with highly polarizable and π-bonding ligands (such as chloride groups and aryl rings) can greatly affect the NMR chemical shifts of reporter groups, so that ignoring their contributions leads to significant over-estimates of the anisotropy due just to the metal-metal bond. We propose a method to quantify and correct for the magnetic anisotropy effects arising from the ligands. Application of this method to $Mo_2(BDAM)_4$ indicates that the magnetic anisotropy of the Mo-Mo quadruple bond in this molecule is about -800×10^{-36} m^3 $molecule^{-1}$. Anisotropies significantly higher than this value (as sometimes reported in the prior literature) are most likely incorrect.

Introduction

When a chemical substance is placed in a uniform magnetic field, its electrons experience a force and respond in such a way as to generate an induced, secondary magnetic field. If the substance has no unpaired electrons, the response has certain characteristics that are denoted by the term diamagnetism.[1] The diamagnetism can be measured in a number of ways, one of which is through the effect of the secondary field on the chemical shifts of NMR active nuclei.[2-7] In the general case the effect of the secondary magnetic field is anisotropic, having different values and signs in different directions depending on the location of the NMR nuclei within the substance. The degree to which the response varies with direction is called the diamagnetic anisotropy of the substance. Measurements of diamagnetic anisotropy find use in structural organic chemistry,[8-10] the characterization of biomaterials in magnetic resonance imaging (MRI),[11-14] and the design of magnetically-responsive materials.[15-17]

The archetypal example of a substance that exhibits diamagnetic anisotropy is benzene: when molecules of benzene are placed in an external magnetic field, it generates a secondary magnetic field that can be thought of classically as the result of the magnetically-induced circulation of the π electrons around the aromatic ring (Figure 1).[18] A similar effect occurs in alkynes,[19] in which (again, in a classical view) the external field causes the π electrons to circulate about the carbon-carbon triple bond axis (Figure 1). Thus, for both arenes and alkynes, nearby nuclei can be either shielded or deshielded by the secondary magnetic field depending on their location with respect to the aromatic ring or C-C triple bond.[20]

Like carbon-carbon multiple bonds, metal-metal multiple bonds also generate secondary magnetic fields, which can similarly be viewed classically as arising from circulation of d-electrons about the bond axis.[21] The diamagnetic anisotropies of these multiple bonds (and in

particular of molybdenum-molybdenum quadruple bonds) have frequently been measured from a combination of solid-state structural data and chemical shifts obtained solution-phase ^{1}H NMR spectra. The diamagnetic anisotropy of the Mo-Mo quadruple bond has been estimated to range from -2112 to -9680 × 10^{-36} m^3 $molecule^{-1}$, or about ten to forty times larger than that of the carbon-carbon triple bond.[21-25]

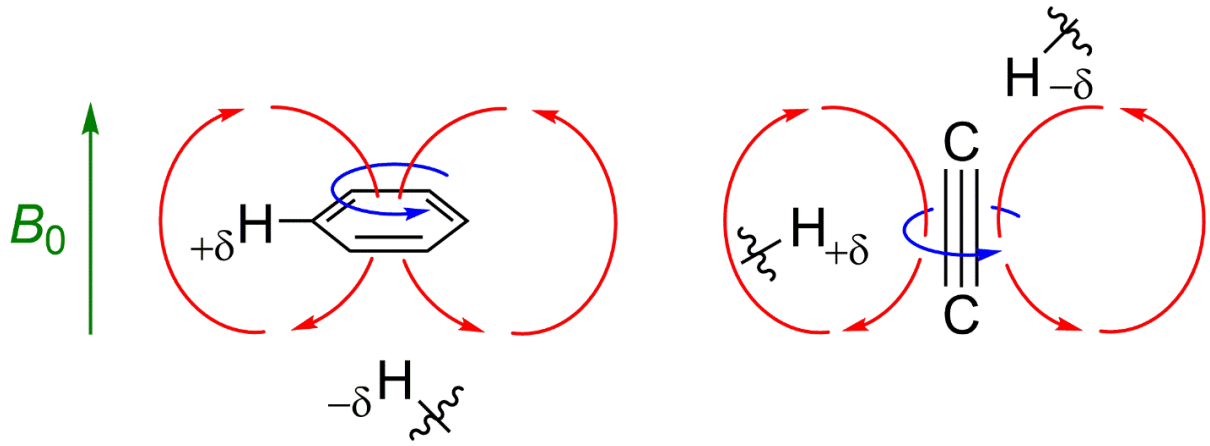

Figure 1. Anisotropies of the magnetic fields (red) generated by the induced currents (blue) of a benzene ring and an alkyne in an external magnetic field (green).

A common assumption in such studies is that the only source of secondary magnetic fields is the metal-metal bond. A few investigators, however, have questioned this assumption. Chisholm studied a series of triply-bonded M_2X_6 compounds of molybdenum and tungsten, where X was an amido or alkoxide ligand, and found that as much as 30% of the chemical shift differences seen in these compounds could be attributed to the secondary magnetic fields arising from metal-ligand π-bonding.[26] In recent work, Berry has pointed out that spin-orbit coupling effects and temperature-independent paramagnetism may contribute significantly to the secondary magnetic fields of compounds that contain metal-metal bonds, so that it is more appropriate to refer to "magnetic anisotropy" rather than "diamagnetic anisotropy".[27]

Computational studies have made it clear that the McConnell "shielding cone" model for the magnetic anisotropies of carbon-carbon single, double, and triple bonds and aromatic rings is an oversimplification, sometimes so much so that the model leads to incorrect predictions. It is a simplification because the shielding cone model ignores other potential effects on the chemical shift of a nucleus, such as electric field effects, orbital interactions, and dispersion between the C-H bonds and the multiple bond.[28] Although for alkynes, McConnell's model qualitatively agrees with the shielding and deshielding regions about the triple bond, the direct effect of the secondary magnetic field on the chemical shifts of nearby protons is actually quite small compared to effects that the model ignores.[28] Whether or not the McConnell shielding cone approximation holds true for metal-metal multiple bonds remains an open question, however, and all studies that use this approximation make an assumption about its validity.

Here, we describe the synthesis and characterization of a new molybdenum(II) dimer $Mo_2(BDAM)_4$, where BDAM is the boranatodimethylaminomethyl group $CH_2NMe_2BH_3$. The BDAM ligand is isoelectronic and isosteric with the neopentyl group, but (unlike neopentyl) the BDAM group can chelate to a metal through both M-C and M-H-B bonds.[29-30] Solid state and solution phase characterization of $Mo_2(BDAM)_4$ has allowed us to estimate the magnetic anisotropy of the Mo-Mo quadruple bond in this compound. We use DFT-based calculations to determine the extent to which the ligands affect the NMR chemical shifts of reporter groups; we find that, in some other dimolybdenum compounds, the ligand-based anisotropies dominate the observed NMR chemical shifts, so that ignoring their contributions leads to significant over-estimates of the anisotropy due just to the metal-metal bond. We propose a method to estimate and correct for the contributions of the ligands to the observed magnetic anisotropy; application of this

method to $Mo_2(BDAM)_4$ suggests that the magnetic anisotropy of the Mo-Mo quadruple bond is ~-800 × 10^{-36} m^3 $molecule^{-1}$.

Results and Discussion

Synthesis of $Mo_2(BDAM)_4$, 1. The addition of 4.5 equiv of $LiCH_2NMe_2BH_3 \cdot thf$[31] (LiBDAM·thf) to $Mo_2(O_2CCF_3)_4$ in diethyl ether at 0 °C rapidly produces a deep red solution from which $Mo_2(BDAM)_4$, **1**, can be isolated by extraction with either pentane or hexanes as a magenta-colored solid in yields of ~10-15%. Compound **1** is air- and moisture-sensitive, moderately soluble in alkanes, and more soluble in diethyl ether, tetrahydrofuran, and toluene. Compound **1** can also be synthesized by addition 4.5 or 3.5 equiv of LiBDAM·thf to $Mo_2(OAc)_4$ or $MoCl_3(thf)_3$, respectively, in diethyl ether, although in lower yields. Solid samples of **1** are stable for days under argon at room temperature; pentane solutions of **1** are stable for weeks at -20 °C but are prone to hydrolysis from trace moisture resulting in the formation of brown precipitate. Compound **1** sublimes under vacuum (< 10 mTorr) at ~80 °C in poor yield; most of the compound decomposes instead.

The infrared spectrum of **1** (Figure S2) displays two strong sets of bands centered at 2380 and 2004 cm^{-1} that can be assigned to terminal B-H and bridging Mo-H-B stretches, respectively.[32] This ~400 cm^{-1} difference, which is similar to the separations seen in the IR spectra of most other transition metal borohydride complexes,[33] indicates that there is a relatively strong interaction between the bridging B-H bonds and the metal center.[30]

Crystallographic Study of $Mo_2(BDAM)_4$, 1. Dark red single crystals of **1** suitable for X-ray diffraction were grown by cooling a concentrated pentane solution to -20 °C. Crystal data and

refinement parameters for **1** are listed in Table S1, and relevant distances and angles are given in Table 1.

Molecules of **1** (Figure 2) reside on crystallographic two-fold axes that bisect the Mo-Mo bond and render the two Mo centers in each molecule symmetry-equivalent. In the crystal structure of **1**, every atom is disordered over two positions with relative site occupancies of 0.782(3) and 0.218(3). In this whole-molecule disorder, the Mo-Mo vectors of the two disordered components intersect at their midpoints to form a 90° angle (Figure S1); similar disordering has been seen in other quadruply-bonded dimers, particularly those with $M_2X_8^{n-}$ and $M_2X_4L_4$ stoichiometries.[34-35] In the following discussion, the metric parameters of only the major component will be described.

Table 1. Selected distances and angles in the major component of $Mo_2(CH_2NMe_2BH_3)_4$, **1**.

Distances (Å)	
Mo(1)-C(1)	2.22(1)
Mo(1)-C(4)	2.21(1)
Mo(1)···B(1)	2.64(1)
Mo(1)-H(1E)	1.95[a]
Mo(1)···B(2)	2.62(1)
Mo(1)-H(2E)	1.88[a]
Mo(1)-Mo(1A)	2.114(2)
Angles (deg)	
C(1)-Mo(1)-H(1E)	79.6[a]
C(4)-Mo(1)-H(2E)	79.7[a]
Mo(1A)-Mo(1)-C(1)	106.0(3)
Mo(1A)-Mo(1)-C(4)	107.6(3)
Mo(1A)-Mo(1)-H(12)	100.1[a]
Mo(1A)-Mo(1)-H(23)	101.7[a]
C(4)-Mo(1)-Mo(1A)-C(4A)	14.5(5)
H(12)-Mo(1)-Mo(1A)-H(12A)	8.5[a]
C(1)-Mo(1)-Mo(1A)-H(23A)	3.9[a]

[a] Estimated standard deviations omitted because hydrogen atoms were placed in idealized positions.

In compound **1**, both of the $CH_2NMe_2BH_3^-$ ligands chelate to a single Mo atom through a Mo-CH_2 bond and a κ^1BH_3-Mo three-center-two-electron interaction; the metal-metal bond is therefore unbridged. The two Mo-CH_2 bonds are mutually *cis*, and each Mo-CH_2 bond is *trans* to a Mo-H-B bond. Like all other M_2L_8 compounds with quadruple bonds, the two ML_4 ligand sets are eclipsed with respect to one another; when compound **1** is viewed along the Mo-Mo vector, there is one pair of eclipsed Mo-CH_2 bonds, one pair of eclipsed Mo-H-B bonds, and two pairs in which a Mo-CH_2 bond eclipses a Mo-H-B bond. The L-Mo-Mo-L torsion angles are 14.5(5)° for the two eclipsed Mo-CH_2 groups, 8.5° for the two eclipsed Mo-H-B bonds, and 3.9° for the eclipsed Mo-CH_2 / Mo-H-B bonds.

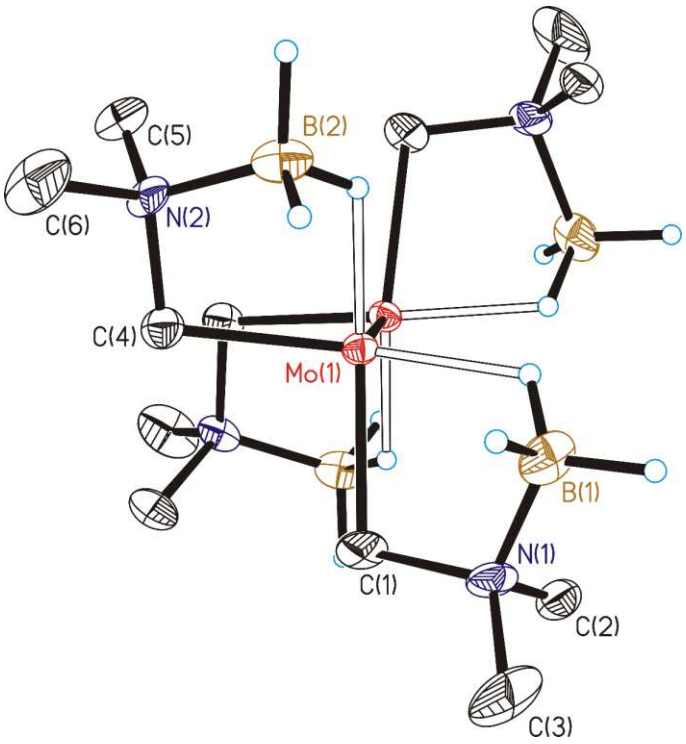

Figure 2. Major component of the molecular structure of $Mo_2(CH_2NMe_2BH_3)_4$, **1**. Ellipsoids are drawn at the 35% probability level, except for the hydrogen atoms, which are represented by arbitrarily sized spheres. Hydrogen atoms bound to carbon have been omitted for clarity.

The Mo-Mo bond length in **1** of 2.114(2) Å is fully consistent with the presence of a quadruple bond: it slightly shorter than those in $Mo_2X_4(diphosphine)_2$ compounds,[23, 36-38] $Mo_2(CH_3)_4(PR_3)_4$[39] compounds, and $Mo_2(CH_3)_8^{4-}$,[40] but slightly longer than that in $Mo_2(OAc)_4$.[41] The average Mo-C bond length in **1** of 2.22(1) Å is ~0.1 Å shorter than those in other molybdenum(II) dimers containing alkyl ligands;[39-40, 42-43] this shortening is likely due to a combination of trans-influence and steric effects. To the best of our knowledge, no other κ^1 borohydride-molybdenum(II) interactions have been structurally characterized. However, the average Mo···B distance in **1** of 2.63(1) Å is ~0.1 Å shorter than that to the bridging κ^1,κ^1-BH_4^- group in the molybdenum(III) dimer $Cp_2Mo_2(\mu\text{-}SMe)_2(\mu\text{-}BH_4)(\mu\text{-}NCHMe)$,[44] and ~0.2 Å shorter than that for the κ^1-BH_4 ligand in the formally molybdenum(0) monomer *trans*-$Mo(BH_4)(NO)(dmpe)_2$.[45] The differences in these Mo···B distances reflect several factors, including the chelating nature of the BDAM ligand, which makes the Mo-H-B angle more acute and thus shortens the Mo···B distance, and the different oxidation states and coordination numbers of these compounds.

Finally, we point out that, despite the whole-molecule disorder, the crystallographically-determined structural model for **1** is chemically quite reasonable: the overall structure is consistent with the NMR spectrum (see below) and all refined bond distances are in excellent agreement with the gas phase DFT structure of **1** optimized at the B3LYP-D3(BJ)/def2-TZVP level of theory (Table S2).

Absorption Spectrum of $Mo_2(BDAM)_4$, 1. The UV-vis absorption spectrum of **1** in Et_2O features a band in the visible region at 537 nm (=18600 cm^{-1}) with a maximum molar absorptivity of 1034 M^{-1} cm^{-1} (Figure 3a). Time-dependent DFT (TPSSh-D3/def2-QZVP) gives a calculated energy for this absorption of 530 nm (18900 cm^{-1}) in good agreement with the experimental value;

the major contribution (79%) to this absorption is a δ → δ* excitation involving the orbitals in the Mo-Mo quadruple bond (Figure 3b and Supporting Information). The energy of the δ → δ* excitation in **1** is similar to that seen for $Mo_2Cl_8^{4-}$ and $Mo_2(CH_3)_8^{4-}$,[46,47] but blue-shifted relative to those seen for $Mo_2X_4(PR_3)_4$ compounds containing four phosphine or two diphosphine ligands and X = alkyl or halide.[23, 37-39] Many factors affect the energies and intensities of δ → δ* excitations in dimolybdenum(II) compounds, including the degree of ionic character and metal-ligand orbital mixing.[21, 48-49]

The absorption spectrum of **1** also contains a weaker band at ~450 nm (22200 cm^{-1}) assignable to the π → δ* excitation and a shoulder at ~350 nm (28600 cm^{-1}) that consists of two overlapping absorptions: one involving metal-to-ligand charge transfer and the other involving ligand-to-metal charge transfer; all these assignments are based on the DFT results (Supporting Information).

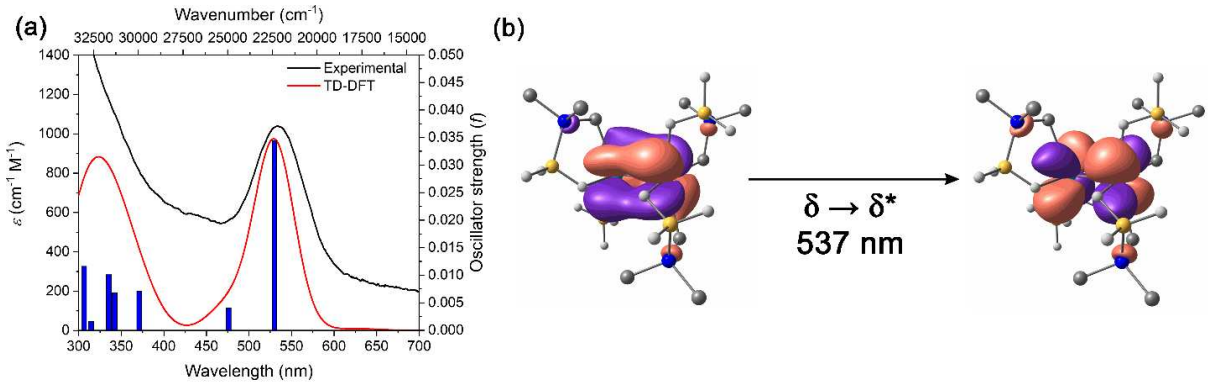

Figure 3. (a) overlay of the experimental (black) and simulated (red) spectra $Mo_2(CH_2NMe_2BH_3)_4$, **1**. (b) Main orbital contributions (contour isovalue = 0.036) to the 537 nm absorption of **1**. TD-DFT calculations were performed at the TPPSh-D3/def2-QZVP level of theory.

Solution Phase NMR Spectra of $Mo_2(BDAM)_4$, 1. All solution phase NMR data of **1** are consistent with its solid-state structure. At room temperature, the magnetic molybdenum(II) dimer

1 is relatively rigid in solution: the ^{1}H NMR spectrum of **1** displays four doublets ($^{2}J_{HH}$ = 11 Hz) corresponding to each of the four diastereotopic CH_2 protons, and four singlets corresponding to each of the four symmetry-inequivalent NMe_2 methyl groups (Figure 4). Of the four CH_2 resonances, two are comparatively deshielded (δ 4.38 and 3.50) whereas the other two are relatively shielded (δ 3.01 and 2.70); the same pattern of two deshielded (δ 2.96 and 2.70) and two shielded (δ 2.21 and 2.19) resonances is seen for the NMe_2 groups. The ^{1}H NMR resonances due to the BH_3 groups of **1** appear as two broad peaks near δ 1.6 and δ 2.2 with relative intensities of 1:2 due to the bridging and terminal B-H sites, respectively (Figure S3).

The significant differences in the chemical shifts of diastereotopic CH_2 protons and NMe_2 methyl groups are attributable to a magnetic anisotropy effect caused (at least in part) by the Mo-Mo quadruple bond in **1**: the secondary magnetic field generated by electrons in the Mo-Mo bond either shields or deshields chemical shifts of nearby protons depending on where they are located within the molecule. If we adopt the customary "shielding cone" model of the through-space NMR shielding effect (see below),[50-51] then the two relatively deshielded methylene and methyl protons of **1** are proximal to the Mo-Mo bond and those that are relatively shielded are distal (Figure 4).

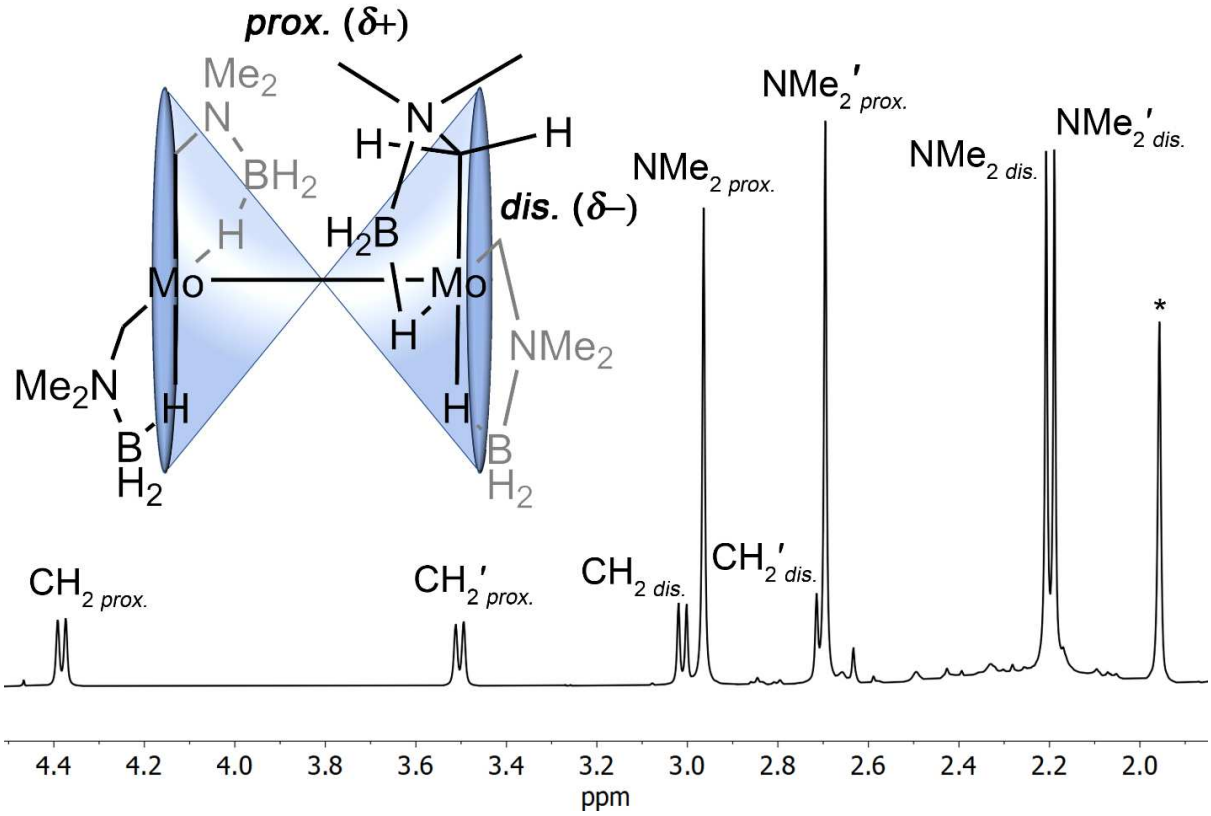

Figure 4. ^{1}H NMR spectrum of $Mo_2(CH_2NMe_2BH_3)_4$, **1**, at room temperature in C_6D_6. Proximal resonances correspond to protons pointing toward the Mo-Mo bond and distal resonances to those pointing away. Primes denote resonances belonging to the same ligand. The peak marked with an asterisk is due to NMe_3BH_3 impurity from trace hydrolysis.

The room temperature $^{13}C\{^{1}H\}$ NMR spectrum of **1** (Figure S4) contains two resonances for the chemically inequivalent methylene groups at δ 70.2 and 66.7 and four resonances for the NMe_2 groups, two near δ 58 and two near δ 53. Contrary to the shielding pattern for proximal and distal protons observed by ^{1}H NMR spectroscopy, the ^{13}C resonances of the proximal methyl groups are shielded in comparison with those for distal methyl groups. This difference in ^{13}C NMR chemical shift ordering for proximal and distal methyl group is likely not an effect of the magnetic anisotropy of the Mo-Mo bond; instead, it almost certainly reflects the much larger contribution from the paramagnetic term in the Ramsey equation for ^{13}C nuclei than for ^{1}H nuclei.[52]

Magnetic Anisotropy of the Mo-Mo Quadruple Bond. The long-range shielding effects of an axially symmetric group of electrons were first treated for carbon-carbon multiple bonds by McConnell[20] and first applied to compounds containing M-M multiple bonds by San Filippo[50] and McGlinchey,[51] and later by others.[22-25] The McConnell model assumes that the magnetic properties of molecules (as measured by their effect on ^{1}H NMR chemical shifts) can be partitioned into contributions from individual bonds. A second assumption made by the McConnell model is that the through-space shielding effect of the multiple bond can be described in terms of a shielding cone, in which hydrogen atoms that are outside the cone (i.e., proximal to the multiple bond) are deshielded and those that are inside the cone (i.e., distal to the multiple bond) are shielded. Both of these assumptions are clearly oversimplifications, but nevertheless the qualitative trends in estimates of the magnetic properties of bonds derived from the McConnell model can still provide meaningful insights.

The shielding cone is a representation of the magnetic anisotropy of the multiple bond, and the latter can be calculated from the NMR chemical shifts of suitable "reporter groups", such as a pair of diastereotopic methylene protons. For an axially symmetric molecule in which the M-M bond axis defines the axis of symmetry, the chemical shift difference ($\Delta\delta$) between a pair of reporter protons A and B is related to the magnetic anisotropy of the M-M bond by the following equation:

$$\Delta\delta = \delta_A - \delta_B = \frac{(\chi_{\parallel} - \chi_{\perp})(G_A - G_B)}{4\pi} \qquad (1)$$

where $\chi_{\parallel}$ and $\chi_{\perp}$ are the magnetic susceptibilities parallel and perpendicular to the M-M bond, respectively. This equation assumes that the reporter nuclei are sufficiently distant that the M-M bond can be regarded as a point dipole.[20] The parameters G_A and G_B, which are geometric terms

that describe the location of protons A and B with respect to the center of the M-M bond, are given by the equation:

$$G = \frac{1-3\cos^2\theta}{3r^3} \quad (2)$$

where r is the distance of the proton to the center of the M-M bond and θ is the acute angle between the vector r and the M-M bond.

For compounds of lower symmetry, equation 1 can be generalized[24] to describe the induced magnetic anisotropy of a M-M bond:

$$\Delta\delta = \delta_A - \delta_B = \frac{(\chi_\parallel - \chi'_\perp)(G'_A - G'_B)}{4\pi} + \frac{(\chi_\parallel - \chi''_\perp)(G''_A - G''_B)}{4\pi} \quad (3)$$

where $\chi'_\perp$ and $\chi''_\perp$ describe the magnetic susceptibilities in two directions perpendicular to the Mo-Mo bond (i.e., in the x and y directions with the Mo-Mo bond vector taken as the z direction). The two perpendicular directions are chosen to coincide with an axis of symmetry for the molecule, if this is possible.[24] The generalized geometric terms G' and G'' are given by equation (2) except that θ is replaced by θ' and θ'', the angles between the vector r and the two directions perpendicular to the Mo-Mo bond.

To use equation 3 to calculate the magnetic anisotropy of a metal-metal bond, two values of δ_A - δ_B must be observable from two pairs of diastereotopic protons. In $Mo_2(CH_2NMe_2BH_3)_4$, **1**, there are two pairs of diastereotopic methyl groups, but their observed chemical shifts – which are the average over three locations owing to rapid rotation – cannot be used in equations 1-3 because the effect of the magnetic anisotropy on chemical shifts is not linear with either r or θ. A better choice of reporter groups are the two pairs of diastereotopic CH_2 protons, each bearing one

hydrogen atom that is proximal to the Mo-Mo bond and one that is distal, and we will use these reporter groups in the present analysis.[53]

For the diastereotopic CH_2 protons, geometric parameters were calculated from the solvent field-corrected DFT-optimized structure of **1** (B3LYP-D3(BJ)/def2-TZVP) to minimize errors associated with the uncertainty of the locations of these hydrogen atoms in the crystal structure; in addition, because the NMR data are taken in solution, the solution structure of **1** almost certainly resembles the calculated solvent-field corrected structure more closely than the solid-state structure, which may be affected by packing forces. Values of $\delta_A - \delta_B$., r, $\theta'_\perp$, $\theta''_\perp$, G', and G'' for the CH_2 protons of **1** are presented in Table 2; the direction of $\chi'_\perp$ for **1** was chosen to coincide with the two-fold rotational axis.

Table 2. Geometric parameters G' and G'' calculated from equations 2 and 4, respectively, for $Mo_2(CH_2NMe_2BH_3)_4$, **1**.

	r (Å)	$\theta'_\perp$ (deg)	$\theta''_\perp$ (deg)	G' ($\times 10^{27}$ m^{-3})	G'' ($\times 10^{27}$ m^{-3})	$\delta_{dis.}$-$\delta_{prox.}$
$CH_{2\ prox.}$	3.124	88.86	18.56	-10.92	18.54	-1.37
$CH_{2\ dis.}$	3.432	86.10	49.37	-8.131	2.243	
$CH_2'_{prox.}$	3.153	20.92	88.87	17.20	-10.62	-0.79
$CH_2'_{dis.}$	3.474	51.36	86.33	1.349	-7.853	

Equations 1 and 3 have been used previously to estimate the magnetic anisotropy induced by the quadruple bonds in various molybdenum(II) dimers; these results are compiled in Table 3.[54] By following the same procedures used in these previous studies (i.e., assuming the McConnell shielding cone approximation is valid), we obtain values of ($\chi_\parallel$ - $\chi'_\perp$) and ($\chi_\parallel$ - $\chi''_\perp$) calculated for **1** (-840 and -1200 $\times 10^{-36}$ m^3 molecule^{-1}, respectively) that are significantly smaller than the range of magnetic anisotropy values calculated for other molybdenum(II) dimers of ca. -(2000–10000) $\times 10^{-36}$ m^3 molecule^{-1}.

We propose that the main reason the magnetic anisotropies calculated for the Mo-Mo quadruple bond in previous studies vary over such a large range is the following: almost all such calculations make the (incorrect) assumption that anisotropic shielding effects due to the ancillary ligands are negligible, and that any chemical shift difference between reporter groups is due solely to the effect of the metal-metal bond. All of the compounds in Table 3 contain ligands such as aryl groups, halides, C=O bonds, and/or C=N bonds, all of which are well-known to produce significant magnetic anisotropy effects.[20, 55-56] Strong evidence in favor of this view is the finding that the values of ($\chi_{\parallel} - \chi_{\perp}$) for the quadruple bond in compounds of the form $Mo_2X_4(dmpm)_2$,where X is a halide,[23] increase in the order F < Cl < Br < I.[20, 55] In addition, some of the molybdenum(II) dimers with the largest values of ($\chi_{\parallel} - \chi_{\perp}$) for the quadruple bond are those that contain both metal-bound halide ligand as well as chelating diphosphine ligands bearing aryl substituents.[24] Some previous studies have recognized that ligand-based anisotropy affects the estimated values of ($\chi_{\parallel} - \chi_{\perp}$) for Mo-Mo multiple bonds.[22-24, 26, 51] In one study, the aryl groups in $Mo_2Cl_4(dpdt)_2$, where dpdt = $Ph_2PCH_2CH_2P(p\text{-}Tol)_2$, were estimated to account for 12% of the total value of ($\chi_{\parallel} - \chi_{\perp}$) of -8800 $\times 10^{-36}$ m^3 $molecule^{-1}$ measured for the Mo-Mo quadruple bond (reducing the value of ($\chi_{\parallel} - \chi_{\perp}$) to -7540 $\times 10^{-36}$ m^3 $molecule^{-1}$).[38]

An additional cause of the large variance in the values of ($\chi_{\parallel} - \chi_{\perp}$) shown in Table 3 is that different methods are used to determine $\Delta\delta$. Arguably the best method is to define $\Delta\delta$ *intramolecularly* as the chemical shift difference between a diastereotopic pair of protons in the molecule[24, 38] (as we have done for **1**). If diastereotopic pairs of protons are not present, previous studies have defined $\Delta\delta$ *intermolecularly* to be the chemical shift of a ligand proton in the multiply-bonded complex referenced to the shift of (1) the free ligand (or a salt thereof),[22-23] (2) an analogous

Ni_2^{4+} dimer,[57-58] or (3) an isostructural dimer containing a dative metal-Lewis acid bond in place of a covalent metal-metal bond.[59]

We point out the intermolecular methods are intrinsically prone to error, but for different reasons depending on the reference chosen: (1) free ligands and ligands bound to a metal can have very different conformations, charge distributions, solvation environments, and local electric fields (leading to different magnetic anisotropies), (2) replacement of the two metal atoms with d^8 Ni^{2+} centers may generate a complex with no metal-metal bond, but magnetic anisotropy may still be present owing to the open-shell nature of the Ni^{2+} centers, (3) interaction between a metal donor and a Lewis acid are highly polarized and could impact the chemical shifts of nearby protons through polarization[59-60] and electric field effects. Finally, we point out that the intramolecular method has its own issues: the chemical shifts of proximal and distal protons could be affected differentially by nearby ligand groups, a topic to which we now turn.

Table 3. Values of $(\chi_{\parallel} - \chi_{\perp})$ (calculated from equation 1) and $(\chi_{\parallel} - \chi'_{\perp})/(\chi_{\parallel} - \chi''_{\perp})$ (calculated from equation 2) for molybdenum(II) dimers (dmpm = bis(dimethylphosphino)methane, Ar = XC_6H_4 with X as *p*-OMe, H , *m*-OMe, *p*-Cl, *m*-Cl, *m*-CF_3, *p*-CF_3, or Ar = 3,5-$Cl_2C_6H_3$, dpdt = 1-(diphenylphosphino)-2-(di-*p*-tolyl-phosphino)ethane, dppe = 1,2-bis(diphenylphosphino)ethane, and dpdbp = l-diphenylphosphino-2-di(*p*-tert-butyl)phenylphosphinoethane).

cmpd	$(\chi_{\parallel} - \chi_{\perp})^a$	$(\chi_{\parallel} - \chi'_{\perp})^a$	$(\chi_{\parallel} - \chi''_{\perp})^a$	ref
$Mo_2(BDAM)_4$[b]	-	-840	-1200	this work
$Mo_2(O_2CCH(OH)C_6H_5)_4$[c]	-2112	-	-	22
$Mo_2(OAc)_4$[c]	-3003	-	-	22
$Mo_2Br_4(dmpm)_2$[c]	-3180	-	-	23
$Mo_2I_4(dmpm)_2$[c]	-5090	-	-	23
$Mo_2(ArNCHNAr)_4$[d]	-(4730-5060)	-	-	57
α-$Mo_2Cl_4(dpdt)_2$[b]	-8800	-8200	-5830	24, 38
α-$Mo_2Cl_4(dppe)_2$[b]	-9680	-9340	-6300	24, 38
α-$Mo_2Cl_4(dpdbp)_2$[b]	-	-9450	-5860	24

[a] Units of $\times 10^{-36}$ m^3 $molecule^{-1}$. [b] Chemical shift difference taken as $\delta_{dis.}$-$\delta_{prox.}$. [c] Chemical shift difference vs free ligand. [d] Chemical shift difference vs analogous $Ni_2(ArNCHAr)_4$ compounds.

Ligand Contributions to Magnetic Anisotropy. Compared with data reported for other compounds using the McConnell shielding cone approximation (Table 3), the values of $\chi_{\parallel} - \chi'_{\perp} = 840 \times 10^{-36}$ m^3 molecule^{-1} and $\chi_{\parallel} - \chi''_{\perp} = -1200 \times 10^{-36}$ m^3 molecule^{-1} determined above for **1** (from the observed ^{1}H NMR chemical shifts and the solvent-field optimized DFT structure) are unusually small. It is notable that **1** contains no highly polarizable or π-bonding ligands, whereas such ligands are commonly found in compounds for which large values have been estimated for the magnetic anisotropy of the metal-metal bond. *We believe that significant errors in estimates of the magnetic anisotropy of metal-metal quadruple bonds arise from the assumption that the ancillary ligands do not affect the chemical shifts of reporter groups*. It is this assumption that we now consider.

One way to cancel out the effect of the ligands, and thereby to obtain more accurate estimates of the magnetic anisotropy of the metal-metal bond, is to compare the NMR chemical shifts of the reporter groups with those of analogous compounds that lack the multiple bond. Any changes in the chemical shifts should be due to the metal-metal bond. Sometimes suitable analogous compounds exist,[59] but many times they do not; the latter case is the situation for compound **1**, for example, as well as many compounds in Table 3. But there still is a way forward: we can compute the ^{1}H NMR spectra of theoretical isostructural compounds in which the metal atoms are replaced with atoms having the same oxidation state and a similar ionic radius and electronegativity, but that have a valence electron count of either d^0 or d^{10} so that there is no metal-metal bond and no open-shell effects.

First, as a check of the accuracy of the DFT NMR calculations, we determined how well they can reproduce the experimental chemical shift differences between the pairs of diastereotopic CH_2 protons in two compounds: our BDAM compound **1**, and the tetraaryldiphosphine complex

$Mo_2Cl_4(dpdt)_2$. For **1**, the two computed Δδ values of 1.44 and 0.99 ppm for the diastereotopic pairs of CH_2 protons are reasonably close to the experimental values of 1.37 and 0.80 ppm. For $Mo_2Cl_4(dpdt)_2$ the computed Δδ value of 1.39 ppm for the diastereotopic phosphine CH_2 protons is very similar to the experimental value of 1.36 ppm.

We then carried out DFT calculations on the d^0 and d^{10} model compounds $M_2(BDAM)_4$ and $M_2Cl_4(dpdt)_2$ where M = Mg^{2+}, Zn^{2+} (see Supporting Information for details). The two ions were substituted into the calculated structure for **1** without allowing the structure to relax. For magnesium, the metal-ligand distances should be almost exactly equal to those that would result if we allowed the structure to optimize: for example, reported Mg-C bond lengths[61-64] (2.120(7)-2.238(9) Å) of terminal alkyl ligands in four-coordinate magnesium(II) complexes are reasonably similar to the Mo-C bond lengths in **1** (2.225(10) and 2.209(10) Å). For zinc, reported Zn-C bond lengths[65-68] (2.007(3)-2.036(2) Å) of terminal alkyl ligands in four-coordinate zinc(II) complexes are shorter than the Mo-C bond lengths in **1** by ca. 0.2 Å, but zinc(II) has an electron count and electronegativity more similar to that of molybdenum(II) than does magnesium(II). Any differences in in the magnetic anisotropy of $Mo_2(BDAM)_4$ and $M_2(BDAM)_4$ (M = Mg, Zn) that arise from differences in metal electronegativity, electron count, or metal-ligand bond lengths should affect the chemical shifts of both proximal and distal protons similarly; thus, these effects are cancelled out when measuring the chemical shift differences Δδ used in equations 1 and 3.

We find that the calculated ^{1}H NMR chemical shift differences Δδ for the two pairs of diastereotopic CH_2 groups in $M_2(BDAM)_4$ are very similar for M = Mg^{2+}or Zn^{2+}, indicating that the use of these metals in model compounds that lack metal-metal bonds is justified; if we take the average over the two metals, the Δδ values are 0.12 and 0.18 ppm (Table S5). Subtracting these numbers from the experimental values of 1.37 and 0.80 ppm seen for **1** gives $\Delta\delta_{corr}$ values of 1.25

and 0.62 ppm; these results show that most of the chemical shift difference between the diastereopic pairs comes from the metal-metal bond. Recalculation of the magnetic anisotropy of the Mo-Mo quadruple bond in **1** from the $\Delta\delta_{corr}$ values gives -680×10^{-36} m^3 $molecule^{-1}$ for ($\chi_{\parallel}$ - $\chi'_{\perp}$) and -1080×10^{-36} m^3 $molecule^{-1}$ for ($\chi_{\parallel}$ - $\chi''_{\perp}$). These anisotropies are only slightly smaller than the uncorrected values of -840 and -1200×10^{-36} m^3 $molecule^{-1}$, respectively. We believe that the small $\Delta\delta$ values seen for the Mg and Zn compounds reflect two aspects of the BDAM ligand: (1) it contains only atoms of relatively low polarizability and (2) it forms bonds (both internally and with the metal) that have purely σ character.

For the model compounds $M_2Cl_4(dpdt)_2$ ($M = Mg^{2+}$, Zn^{2+}), the average calculated ^1H NMR chemical shift difference $\Delta\delta$ between the proximal and distal CH_2 protons (see Supporting Information for details) is 1.46 ppm (Table S5); interestingly, this value is slightly *larger* than the experimental value[24] of 1.36 ppm. This result indicates that nearly all of the chemical shift difference seen for the reporter CH_2 groups in $Mo_2Cl_4(dpdt)_2$ (which was previously ascribed as being solely due to the magnetic anisotropy of the Mo-Mo bond) actually arises from the ligands. We do not mean to imply that the magnetic anisotropy of the Mo-Mo bond in this compound is zero, but only that the chemical shifts of the reporter protons are dominated by effects from nearby aryl and chloride groups. This result also likely applies to the other compounds in Table 3 that contain aryl and halide groups.

Identifying Ancillary Sources of Magnetic Anisotropy. We can also utilize DFT to tease apart to what extent the different ligands contribute to the chemical shift differences seen for reporter groups. Specifically, for $Mo_2Cl_4(dpdt)_2$ we were interested to determine the relative importance of (1) the aryl groups on the phosphine and (2) the halide groups attached to molybdenum. We therefore carried out DFT NMR analyses of the theoretical model compounds

$Mo_2H_4(dpdt)_2$, $Mo_2Cl_4(PH_2CH_2CH_2PH_2)_2$, and $Mo_2H_4(PH_2CH_2CH_2PH_2)_2$ (Table S5). In these models, the potential ligand-based sources of magnetic anisotropy are systematically replaced with σ-only-interacting hydrogen atoms; the comparison of the computed values of Δδ for these model compounds with that of $Mo_2Cl_4(dpdt)_2$ should reveal the extent to which each ligand group affects the magnetic anisotropy experienced by the reporter CH_2 groups.

The computed values of Δδ for $Mo_2H_4(dpdt)_2$ and $Mo_2Cl_4(PH_2CH_2CH_2PH_2)_2$ of 0.32 and 1.09 ppm, respectively, (vs. 1.36 ppm observed experimentally for $Mo_2Cl_4(dpdt)_2$) suggest that the chloride ligands in $Mo_2Cl_4(dpdt)_2$ affect the chemical shifts of proximal and distal CH_2 protons more significantly than the aryl rings.[69]

Interestingly, the computed chemical shifts of the proximal protons in $Mo_2H_4(PH_2CH_2CH_2PH_2)_2$ (in which both major ancillary sources of magnetic anisotropy have been replaced with hydrogen atoms) are more shielded than those of the distal protons, resulting in a Δδ of -0.38 ppm (Table S5). The oppositely-signed value of Δδ suggests that the methylene protons of the bis(phosphino)ethylene ligands in *α*-$Mo_2X_4(LL)_2$ compounds are too far away from the Mo-Mo bond for the magnetic anisotropy of that bond to dominate their chemical shifts. This result agrees with the finding above that the chemical shifts of the reporter protons in $Mo_2Cl_4(dpdt)_2$ are dominated by effects from aryl and chloride groups. In the DFT optimized structure of $Mo_2Cl_4(dpdt)_2$, the proximal and distal protons are on average 3.71 and 4.69 Å away from the Mo-Mo centroid, respectively (compared with 3.14 and 3.46 Å for the proximal and distal protons of **1**, respectively). Not surprisingly, the effect of the magnetic anisotropy of a metal-metal multiple bonds on the chemical shifts of reporter protons tends to zero as the protons are farther from the metal-metal bond.

Conclusions.

A new compound containing a molybdenum-molybdenum quadruple bond has been synthesized and characterized, $Mo_2(CH_2NMe_2BH_3)_4$, **1**, in which each molybdenum center is bound to two chelating boranatodimethylaminomethyl (BDAM) ligands. In both the solid state and solution, the diastereotopic CH_2 groups of **1** are positioned with one proton proximal to the Mo-Mo bond and one proton distal. We have used the chemical shifts of these diastereotopic protons, in combination with the McConnell shielding cone model, to estimate the magnetic anisotropy of the Mo-Mo multiple bond. Although the McConnell model assumes (simplistically) that the magnetic properties of a molecule can be dissected into contributions from individual bonds, and that the shielding caused by a multiple bond has the geometric properties of a cone, nevertheless it provides some useful insights and – with appropriate care – can be used to compare one molecule with another, within the context of the model. It is the issue of appropriate care that we consider here.

In almost all other studies of the application of the McConnell model to determine the magnetic anisotropy of metal-metal multiple bonds, it has been assumed that one may ignore any influence of the ancillary ligands on the chemical shifts of the reporter groups.. But here we have shown that this assumption is not a good one, and that making it can lead to significant errors. A DFT-based correction for the effect of the BDAM ligands on the chemical shifts of proximal and distal CH_2 protons in **1** was performed by simulating the NMR spectra of model compounds $M_2(BDAM)_4$ (M = Mg, Zn) which do not feature a M-M bond. After correcting for the effect of the ligands in **1**, we find that ($\chi_{\parallel} - \chi'_{\perp}$) and ($\chi_{\parallel} - \chi''_{\perp}$) due to the metal-metal quadruple bond are -680 and -1080 × 10^{-36} m^3 $molecule^{-1}$, respectively. Application of the same correction method to the tetraaryldiphosphine complex $Mo_2Cl_4(dpdt)_2$ (which has reported values of -8200 and -5830 ×

10^{-36} m^3 $molecule^{-1}$ for ($\chi_{\parallel}$ - $\chi'_{\perp}$) and ($\chi_{\parallel}$ - $\chi''_{\perp}$), respectively) demonstrates that essentially all of the difference in chemical shift between the proximal and distal CH_2 protons of the phosphine ligands is due to the shielding effects of the aryl and halide groups. As a result, the -8200 and -5830 × 10^{-36} m^3 $molecule^{-1}$ are significant overestimates of the true values of the magnetic anisotropy of the metal-metal bond in that compound.

In order to determine to tease apart to what extent the ligands give rise to the chemical shift differences seen for reporter groups in compounds containing multiple bonds, we carried out DFT NMR calculations on analogs of $Mo_2Cl_4(dpdt)_2$ in which the chloride groups or aryl rings (or both) were replaced with magnetically innocent hydrogen atoms. These calculations suggest that the chemical shifts of proximal and distal protons in $Mo_2Cl_4(dpdt)_2$ are affected most significantly by the chloride groups, to a lesser extent by the aryl rings on the phosphine ligands, and almost not at all by the magnetic anisotropy of the metal-metal bond. This conclusion results from the fact that proximal and distal protons in $Mo_2Cl_4(dpdt)_2$ and related compounds are relatively far away from the Mo-Mo bond, so that their chemical shifts are almost insensitive to the magnetic anisotropy of that bond.

We have shown here that in some cases it is possible to correct for the magnetic effects of ligand groups, and thereby enable more meaningful comparisons of the magnetic anisotropies of metal-metal bonds. This work shows that it is often a significant mistake to ignore the effects of ligand groups on the chemical shifts of reporter groups, and presents what we believe is a better estimate of the magnetic anisotropy of the Mo-Mo quadruple bond: ~-800 × 10^{-36} m^3 $molecule^{-1}$.. The methods presented in this study to quantify ancillary ligand-effects on chemical shifts should be applicable to a wide range of molecular structures and should enable better understandings of the responses of common chemical groups to an external magnetic field.

Experimental Section

All manipulations were carried out under argon or in vacuum using standard Schlenk and glovebox techniques unless otherwise specified. All glassware was oven-dried before use, assembled hot, and cooled under vacuum. Solvents were dried over 3 Å molecular sieves (hexanes), or distilled under nitrogen from sodium/benzophenone (pentane, diethyl ether, and tetrahydrofuran) or sodium (toluene), and sparged with argon immediately before use. LiBDAM·thf[31], $Mo_2(O_2CCF_3)_4$[70], $Mo_2(OAc)_4$[71], and $MoCl_3(thf)_3$[72] were synthesized by literature procedures. Benzene-d_6 (Cambridge Isotope Laboratories) was distilled from calcium hydride under argon and stored over 3 Å molecular sieves.

Elemental analyses were carried out by the University of Illinois Microanalytical Laboratory. FTIR spectra were acquired on a Thermo Nicolet IR200 spectrometer as mineral oil mulls between KBr plates and processed using the OMNIC^{TM} software package with automatic baseline corrections. UV-vis absorption spectra were acquired on a Varian Cary 60 spectrophotometer in a 1 cm borosilicate Schlenk cuvette. The ^{1}H and $^{13}C\{^{1}H\}$ NMR data were collected on a B600 Bruker NEO instrument at 14.1 T, and the ^{11}B and $^{11}B\{^{1}H\}$ NMR data were collected on a Varian Unity Inova 400 instrument at 9.4 T. Chemical shifts are reported in δ units (positive shifts to high frequency) relative to $SiMe_4$ (^{1}H, ^{13}C) by assigning appropriate shifts to solvent peaks, or to an external standard of $BF_3·Et_2O$ (^{11}B) by sample replacement. X-ray crystallographic data were collected by the staff of the G. L. Clark X-ray Laboratory at the University of Illinois.

Tetrakis(boranatodimethylaminomethyl)dimolybdenum(II). $Mo_2(CH_2NMe_2BH_3)_4$, 1. To a stirred solution of $Mo_2(O_2CCF_3)_4$ (290 mg, 0.45 mmol) in diethyl ether (20 mL) at 0 °C was added dropwise a solution of $LiCH_2NMe_2BH_3$·thf (300 mg, 1.91 mmol) in diethyl ether (20 mL). The mixture was stirred for 1.5 h at 0 °C to afford a deep red homogeneous solution. The mixture was taken to dryness under vacuum at room temperature to afford a red-brown residue which was extracted with pentane (4 × 40 mL) yielding a magenta solution and dark solids. The solution was filtered and the filtrate was taken to dryness under vacuum to afford a red microcrystalline powder Yield: 20 mg (9%). Anal. Calc. for $Mo_2N_4C_{12}B_4H_{44}$: C, 30.1; H, 9.3; N, 11.7. Found: C, 30.0; H, 8.7; N, 10.6. The low values of H and N content are consistent with the presence of small amounts of trifluoroacetate groups, but no signal for this species could be detected by ^{19}F NMR spectroscopy. ^1H NMR (C_6D_6, 25 °C, 600.1 MHz): δ 4.38 (d, $^2J_{HH}$ = 11 Hz, 1 H, $CH_{2\ prox}$), 3.50 (d, $^2J_{HH}$ = 11 Hz, 1 H, $CH_{2\ prox}$), 3.01 (d, $^2J_{HH}$ = 11 Hz, 1 H, $CH_{2\ dis}$), 2.96 (s, 3 H, $NMe_{2\ prox}$), 2.70 (d, $^2J_{HH}$ = 11 Hz, 1 H, $CH_{2\ dis}$), 2.70 (s, 3 H, $NMe_{2\ prox}$), 2.24 (m, 8 H, B-H_{term}), 2.21 (s, 3 H, $NMe_{2\ dis}$), 2.19 (s, 3 H, $NMe_{2\ dis}$), 1.59 (br q, 4 H, B-H_{bridg}). $^{13}C\{^1H\}$ NMR (C_6D_6, 25 °C, 150.9 MHz): δ 70.2 (s, CH_2), 66.7 (s, CH_2), 58.2 (s, $NMe_{2\ dis}$), 57.4 (s, $NMe_{2\ dis}$), 53.5 (s, $NMe_{2\ prox}$), 52.4 (s, $NMe_{2\ prox}$). ^{11}B NMR (C_6D_6, 25 °C, 128.4 MHz): δ -14.9 (s, fwhm = 300 Hz, BH_3). IR (cm^{-1}): 2380 s, 2308 m, 2272 sh, 2225 w, 2044 m, 2004 m, 1973 m, 1855 w, 1403 w, 1261 s, 1230 w, 1165 m, 1124 sh, 1107 s, 1093 sh, 1018 s, 984 s, 800 s. Single crystals suitable for X-ray diffraction were grown by cooling a saturated pentane solution to -20 °C.

Computational Details. Structural optimizations, frequency calculations, TD-DFT, and NMR calculations were performed with the Orca 5.0.3 program.[73-74] All geometry optimizations employed Grimme's D3 empirical dispersion correction[75] applied with Becke-Johnson (BJ) damping.[76] Geometry optimizations and frequency calculations of **1**, $Mo_2H_4(PH_2CH_2CH_2PH_2)$,

and $Mo_2Cl_4(PH_2CH_2CH_2PH_2)_2$ were performed using the B3LYP functional[77-78] and the def2-TZVP[79-80] basis set for all atoms. Geometry optimizations and frequency calculations of $Mo_2Cl_4(dpdt)_2$ and $Mo_2H_4(dpdt)_2$ were performed using the B3LYP functional, the def2-TZVP basis set for Mo atoms, and the def2-SVP[80] basis set for all other atoms. The optimizations of $Mo_2H_4(dpdt)_2$, $Mo_2Cl_4(PH_2CH_2CH_2PH_2)_2$, and $Mo_2H_4(PH_2CH_2CH_2PH_2)_2$ were performed by substituting H atoms for appropriate groups in the optimized structure of $Mo_2Cl_4(dpdt)_2$ and refining only the locations of the newly added H atoms. TD-DFT calculations of **1** were performed using the TPSSh functional,[81] the def2-QZVP basis set,[79-80, 82] and Grimme's D3 empirical dispersion correction with BJ damping. Solvent field corrections were employed using the conductor-like polarizable continuum model[83] with default parameters for benzene or dichloromethane.

The functionals and basis sets used for geometry optimizations were chosen based on their ability to reproduce the crystallographically-determined structures of other transition metal compounds that contain boranatodimethylamino groups.[30] Functionals and basis sets used for TD-DFT calculations were chosen based on their ability to reproduce absorption spectra (Table S3).

Acknowledgments

G.S.G. thanks the National Science Foundation under grant CHE 19-54745 for support of this research, and the School of Chemical Sciences of the University of Illinois for computational resources.

ASSOCIATED CONTENT

Supporting Information Available

Crystallographic study of compound **1**, IR, ^{1}H, $^{13}C\{^{1}H\}$, ^{11}B, and $^{11}B\{^{1}H\}$ NMR spectra of **1**, absorption spectra analysis of **1**, DFT calculations of ^{1}H NMR chemical shifts of $Mo_2(CH_2NMe_2BH_3)_4$ (1) and $Mo_2Cl_4(dpdt)_2$ (PDF), and coordinates of computationally optimized structures (XYZ).

Accession Codes

CCDC 2323737 contains the supplementary crystallographic data for this paper. These data can be obtained free of charge via www.ccdc.cam.ac.uk/data_request/cif, or by emailing data_request@ccdc.cam.ac.uk, or by contacting The Cambridge Crystallographic Data Centre, 12 Union Road, Cambridge CB2 1EZ, UK; fax: +44 1223 336033

AUTHOR INFORMATION

Corresponding Author

* E-mail: girolami@scs.illinois.edu (G.S.G).

Author Contributions

All authors have given approval to the final version of the manuscript.

Funding Sources

National Science Foundation under grant CHE 1954745 (to G.S.G.).

References

1. Bothner-By, A. A.; Pople, J. A., Diamagnetic Anisotropy of Electron Groups. *Annu. Rev. Phys. Chem.* **1965,** *16*, 43-66.
2. Mahoney, J. M.; Stucker, K. A.; Jiang, H.; Carmichael, I.; Brinkmann, N. R.; Beatty, A. M.; Noll, B. C.; Smith, B. D., Molecular Recognition of Trigonal Oxyanions Using a Ditopic Salt Receptor: Evidence for Anisotropic Shielding Surface around Nitrate Anion. *J. Am. Chem. Soc.* **2005,** *127*, 2922-2928.
3. Mallick, S.; Lu, Y.; Luo, M. H.; Meng, M.; Tan, Y. N.; Liu, C. Y.; Zuo, J.-L., Aromaticity-driven Molecular Structural Variation and Electronic Configuration Alternation: An Example of Cyclic π Conjugation Involving a Mo–Mo δ Bond. *Inorg. Chem.* **2017,** *56*, 14888-14899.
4. McGlinchey, M. J.; Nikitin, K., Direct Measurement of the Diamagnetic Anisotropy of the Ferrocenyl Moiety: The Origin of Unusual ^{1}H NMR Shifts in Ferrocenyl-triptycenes and Barrelenes. *J. Organomet. Chem.* **2014,** *751*, 809-814.
5. Peeks, M. D.; Claridge, T. D. W.; Anderson, H. L., Aromatic and Antiaromatic Ring Currents in a Molecular Nanoring. *Nature* **2017,** *541*, 200-203.
6. Sindkhedkar, M. D.; Mulla, H. R.; Cammers-Goodwin, A., Three-state, Conformational Probe for Hydrophobic, π-Stacking Interactions in Aqueous and Mixed Aqueous Solvent Systems: Anisotropic Solvation of Aromatic Rings. *J. Am. Chem. Soc.* **2000,** *122*, 9271-9277.
7. Tanaka, S.; Sugihara, Y.; Sakamoto, A.; Ishii, A.; Nakayama, J., The Thiosulfinyl Group Serves as a Stereogenic Center and Shows Diamagnetic Anisotropy Similar to That of the Sulfinyl Group. *J. Am. Chem. Soc.* **2003,** *125*, 9024-9025.
8. Camp, A. M.; Kita, M. R.; Grajeda, J.; White, P. S.; Dickie, D. A.; Miller, A. J. M., Mapping the Binding Modes of Hemilabile Pincer–Crown Ether Ligands in Solution Using Diamagnetic Anisotropic Effects on NMR Chemical Shift. *Inorg. Chem.* **2017,** *56*, 11141-11150.
9. Harada, N., Determination of Absolute Configurations by Electronic CD Exciton Chirality, Vibrational CD, ^{1}H NMR Anisotropy, and X-ray Crystallography Methods – Principles, Practices, and Reliability. In *Structure Elucidation in Organic Chemistry*, 2015; pp 393-444.
10. Henen, M. A.; Hamdi, A.; Farahat, A. A.; Massoud, M. A. M., Understanding Chemistry and Unique NMR Characters of Novel Amide and Ester Leflunomide Analogues. *Magnetochemistry* **2017,** *3*, 41.
11. Hänninen, N.; Rautiainen, J.; Rieppo, L.; Saarakkala, S.; Nissi, M. J., Orientation Anisotropy of Quantitative MRI Relaxation Parameters in Ordered Tissue. *Sci. Rep.* **2017,** *7*, 9606.
12. Dibb, R.; Xie, L.; Wei, H.; Liu, C., Magnetic Susceptibility Anisotropy Outside the Central Nervous System. *NMR Biomed.* **2017,** *30*, e3544.
13. Lee, J.; Shmueli, K.; Fukunaga, M.; van Gelderen, P.; Merkle, H.; Silva, A. C.; Duyn, J. H., Sensitivity of MRI Resonance Frequency to the Orientation of Brain Tissue Microstructure. *Proc. Natl. Acad. Sci.* **2010,** *107*, 5130-5135.
14. Wang, Y.; Liu, T., Quantitative Susceptibility Mapping (QSM): Decoding MRI Data for a Tissue Magnetic Biomarker. *Magn. Reson. Med.* **2015,** *73*, 82-101.
15. Naga, N.; Saito, Y.; Noguchi, K.; Takahashi, K.; Watanabe, K.; Yamato, M., Magnetic-field-induced Alignment of Syndiotactic Polystyrene. *Polym. J.* **2016,** *48*, 709-714.
16. Rešetič, A.; Milavec, J.; Zupančič, B.; Domenici, V.; Zalar, B., Polymer-dispersed Liquid Crystal Elastomers. *Nat. Commun.* **2016,** *7*, 13140.

17. Sklute, E. C.; Eguchi, M.; Henderson, C. N.; Angelone, M. S.; Yennawar, H. P.; Mallouk, T. E., Orientation of Diamagnetic Layered Transition Metal Oxide Particles in 1-Tesla Magnetic Fields. *J. Am. Chem. Soc.* **2011,** *133*, 1824-1831.
18. Pauling, L., The Diamagnetic Anisotropy of Aromatic Molecules. *J. Chem. Phys.* **1936,** *4*, 673-677.
19. Reddy, G. S.; Goldstein, J. H., Diamagnetic Anisotropy Effects of C≡C and C≡N Bonds in Nuclear Magnetic Resonance Spectroscopy. *J. Chem. Phys.* **1963,** *39*, 3509-3512.
20. McConnell, H. M., Theory of Nuclear Magnetic Shielding in Molecules. I. Long-Range Dipolar Shielding of Protons. *J. Chem. Phys.* **1957,** *27*, 226-229.
21. Cotton, F. A., Physical, Spectroscopic, and Theoretical Results. In *Multiple Bonds Between Metal Atoms*, 3 ed.; Cotton, F. A.; Murillo, C. A.; Walton, R. A., Eds. Springer Science and Business Media, Inc.: 2005.
22. Agaskar, P. A.; Cotton, F. A., Diamagnetic Anisotropy of the Mo≡Mo Bond in $Mo_2(O_2CR)_4$ Type Complexes. *Polyhedron* **1986,** *5*, 899-900.
23. Cotton, F. A.; Dunbar, K. R.; Hong, B.; James, C. A.; Matonic, J. H.; Thomas, J. L. C., Complexes Containing Heteronuclear and Homonuclear Quadruple Bonds. Preparation and Characterization of Bis[bis(dimethylphosphino)methane]tetrachloromolybdenumtungsten and $Mo_2X_4(dmpm)_2$ (X = Bromide, Iodide). *Inorg. Chem.* **1993,** *32*, 5183-5187.
24. Cotton, F. A.; Kitagawa, S., Diamagnetic Anisotropy of Quadruple Mo≡Mo Bonds: *α*-$Mo_2Cl_4(diphosphine)_2$ Complexes. *Polyhedron* **1988,** *7*, 1673-1676.
25. Abraham, R. J.; Reid, M., Proton Chemical Shifts in NMR. Part 16.1 Proton Chemical Shifts in Acetylenes and the Anisotropic and Steric Effects of the Acetylene Group. *J. Chem. Soc., Perkin Trans.* **2001**, 1195-1204.
26. Blatchford, T. P.; Chisholm, M. H.; Huffman, J. C., Diamagnetic Anisotropy of M≡M Bonded Molecules for M = Mo or W: Mow Much π is There and How Do We Slice It? *Polyhedron* **1987,** *6*, 1677-1680.
27. Sunderland, T. L.; Berry, J. F., Metal–Metal Single Bonds with the Magnetic Anisotropy of Quadruple Bonds: A Systematic Series of Heterobimetallic Bismuth(II)–Rhodium(II) Formamidinate Complexes. *Chem. Eur. J.* **2016,** *22*, 18564-18571.
28. Baranac-Stojanović, M., New Insight into the Anisotropic Effects in Solution-state NMR Spectroscopy. *RSC Adv.* **2014,** *4*, 308-321.
29. Lastowski, R. J.; Caroff, C. M.; Vogiatzis, K. D.; Girolami, G. S., Synthesis and Characterization of Chelating Alkyl-borohydride Complexes of Thorium and Uranium: $Th(CH_2NMe_2BH_3)_4$ and $U(CH_2NMe_2BH_3)_4$. *Organometallics* **2023,** *42*, 2839-2848.
30. Lastowski, R. J.; Yarranton, J. T.; Zhu, L.; Vogiatzis, K. D.; Girolami, G. S., Three-Center M–H–B Bonds Are Strong Field Interactions. Synthesis and Characterization of $M(CH_2NMe_2BH_3)_3$ Complexes of Titanium, Chromium, and Cobalt. *J. Am. Chem. Soc.* **2023,** *145*, 23585-23599.
31. Betley, T. A.; Peters, J. C., Synthesis of the (Dialkylamino)borate, $[Ph_2B(CH_2NMe_2)_2]^-$, Affords Access to N-Chelated Rhodium(I) Zwitterions. *Inorg. Chem.* **2002,** *41*, 6541-6543.
32. Daly, S. R.; Kim, D. Y.; Girolami, G. S., Lanthanide *N*,*N*-Dimethylaminodiboranates as a New Class of Highly Volatile Chemical Vapor Deposition Precursors. *Inorg. Chem.* **2012,** *51*, 7050-7065.
33. Viktor, D. M., Structural and Dynamic Properties of Tetrahydroborate Complexes. *Russ. Chem. Rev.* **2000,** *69*, 727.

34. Gross, C. L.; Wilson, S. R.; Girolami, G. S., Synthesis and Characterization of $[(C_5Me_5)_2OsH]_2[Os_2Br_8]$. The Eclipsed Rotamer of the Triply-Bonded $Os_2Br_8^{2-}$ Anion. *Inorg. Chem.* **1995,** *34*, 2582-2586.
35. Cotton, F. A.; Eglin, J. L., Crystallographic Disorder in $[M_2X_8]^{n-}$, $M_2X_4L_4$ and Related Compounds: Chemical and Theoretical Implications. *Inorganica Chim. Acta* **1992,** *198-200*, 13-22.
36. Agaskar, P.; Cotton, F. A., Preparation of the Crystalline *β* (bridged) Isomer of $Mo_2Cl_4(dppe)_2$ and Determination of its Crystal Structure. *Inorg. Chem.* **1984,** *23*, 3383-3387.
37. Chen, J.-D.; Cotton, F. A.; DeCanio, E. C., Syntheses, Structures and Spectra of *β*-$Mo_2X_4(dpcp)_2$ (X=Cl, Br, I), where dpcp is (±) -*trans*-1,2-bis(diphenylphosphino)cyclopentane. A Study of Several Interesting Effects of Halogen Atoms on the Mo≣Mo Quadruple Bond. *Inorganica Chim. Acta* **1990,** *176*, 215-223.
38. Cotton, F. A.; Kitagawa, S., Preparation, Spectroscopic Properties, and Characterization of *anti*- and *syn*-*α*-$Mo_2Cl_4[(C_6H_5)_2PCH_2CH_2P(p\text{-}CH_3C_6H_4)_2]$ in Solution and in the Solid State. *Inorg. Chem.* **1987,** *26*, 3463-3468.
39. Cotton, F. A.; Wiesinger, K. J., Structures of $Mo_2(CH_3)_4(PR_3)_4$ Molecules: Constancy of Covalent Radius of Molybdenum in these and other $Mo_2X_4(PR_3)_4$ Molecules. *Inorg. Chem.* **1990,** *29*, 2594-2599.
40. Cotton, F. A.; Troup, J. M.; Webb, T. R.; Williamson, D. H.; Wilkinson, G., Preparation, Chemistry, and Structure of the Lithium Salt of the Octamethyldimolybdate(II) Ion. *J. Am. Chem. Soc.* **1974,** *96*, 3824-3828.
41. Cotton, F. A.; Mester, Z. C.; Webb, T. R., Dimolybdenum Tetraacetate. *Acta Crystallogr. B* **1974,** *30*, 2768-2770.
42. Hursthouse, M. B.; Malik, K. M. A., Di-*μ*-acetato-bis[(trimethylphosphine)(trimethylsilylmethyl)molybdenum(II)] (Mo-Mo). *Acta Crystallogr. B* **1979,** *35*, 2709-2712.
43. Beshouri, S. M.; Fanwick, P. E.; Rothwell, I. P., Synthesis and Solid State Structure of Bis(*μ*-acetate)bis(*p*-methylbenzyl)bis(trimethylphosphine)-dimolybdenum (Mo≣Mo), $Mo_2(O_2CCH_3)_2(CH_2Ph\text{-}p\text{-}Me)_2(PMe_3)_2$. *Inorganica Chim. Acta* **1987,** *129*, 87-90.
44. Cabon, N.; Pétillon, F. Y.; Schollhammer, P.; Talarmin, J.; Muir, K. W., Reaction of BH_4^- with $\{Mo_2Cp_2(\mu\text{-}SMe)\}$ Species to Give Tetrahydroborato, Hydrido or Dimetallaborane Compounds: Control of Product by Ancillary Ligands. *Dalton Trans.* **2004**, 2708-2719.
45. Liang, F.; Schmalle, H. W.; Fox, T.; Berke, H., Hydridic Character and Reactivity of Di[1,2-bis-(dimethylphosphino)ethane]hydridonitrosylmolybdenum(0). *Organometallics* **2003,** *22*, 3382-3393.
46. Norman, J. G., Jr.; Kolari, H. J., Electronic Structure of Octachlorodimolybdate(II). *J. Am. Chem. Soc.* **1975,** *97*, 33-37.
47. Sattelberger, A. P.; Fackler, J. P., Spectral Studies of Octamethyldimetalates of Molybdenum(II), Rhenium(III), and Chromium(II). The Assignment of the δ→δ* Transition. *J. Am. Chem. Soc.* **1977,** *99*, 1258-1259.
48. Templeton, J. L., Metal-Metal Bonds of Order Four. In *Prog. Inorg. Chem.*, 1979; pp 211-300.
49. Hopkins, M. D.; Gray, H. B.; Miskowski, V. M., δ→δ* Revisited: What the Energies and Intensities Mean. *Polyhedron* **1987,** *6*, 705-714.
50. San Filippo, J., Diamagnetic Anisotropy Induced by Metal-Metal Multiple Bonds. *Inorg. Chem.* **1972,** *11*, 3140-3143.

51. McGlinchey, M. J., Diamagnetic Anisotropy of Metal-Metal Triple Bonds. *Inorg. Chem.* **1980,** *19*, 1392-1394.
52. Jameson, C. J.; Gutowsky, H. S., Calculation of Chemical Shifts. I. General Formulation and the Z Dependence. *J. Chem. Phys.* **1964,** *40*, 1714-1724.
53. In using the diastereotopic CH_2 groups as the reporters, we should keep in mind that the McConnell shielding cone model is based on the "long-range" approximation that the distance to the reporter groups is much greater than the size of the chemical group that generates the anisotropy (in this case, the M-M bond). Most workers have adopted McConnell's original suggestion that a given proton will be considered to be at long-range if the shielding field does not arise from the chemical bond that holds the proton to its host molecule. This definition certainly applies to the diastereotopic CH_2 groups in the present molecule. But these CH_2 protons lie between 3.12 and 3.47 Å from the center of the M-M bond, whereas the M-M bond length is 2.114(2) Å, corresponding to a ratio of about 1.5. At such a small ratio, the mathematical requirements of the long-range approximation are poorly met, so that magnetic anisotropy deduced for **1** from McConnell's equation is best regarded as an "effective magnetic anisotropy". Nevertheless, we should still be able to compare our values with those (based on the same assumption) of other compounds that contain M-M multiple bonds.
54. Across different studies, values of $(\chi_{\parallel} - \chi_{\perp})$ are calculated either with or without the inclusion of the steradian factor of 4π. We have chosen in this study to include the steradian as shown in equations 1, 2, and 3; accordingly, all previously reported values of $(\chi_{\parallel} - \chi_{\perp})$ that do not include the steradian were converted.
55. Goldstein, J. H.; Reddy, G. S., Empirical Method for Estimating Diamagnetic Anisotropy Effects in NMR Spectroscopy, Based upon the Use of C^{13}–H Coupling Constants. *J. Chem. Phys.* **1962,** *36*, 2644-2647.
56. Pople, J. A., Proton Magnetic Resonance of Hydrocarbons. *J. Chem. Phys.* **1956,** *24*, 1111-1111.
57. Lin, C.; Protasiewicz, J. D.; Smith, E. T.; Ren, T., Linear Free Energy Relationships in Dinuclear Compounds. 2. Inductive Redox Tuning *via* Remote Substituents in Quadruply Bonded Dimolybdenum Compounds. *Inorg. Chem.* **1996,** *35*, 6422-6428.
58. Cotton, F. A.; Ren, T., Preparation and Characterization of Two New Group VI Quadruply Bonded Dinuclear Compounds: $Cr_2(DFM)_4$ and $W_2(DFM)_4$. *J. Am. Chem. Soc.* **1992,** *114*, 2237-2242.
59. Eisenhart, R. J.; Rudd, P. A.; Planas, N.; Boyce, D. W.; Carlson, R. K.; Tolman, W. B.; Bill, E.; Gagliardi, L.; Lu, C. C., Pushing the Limits of Delta Bonding in Metal–Chromium Complexes with Redox Changes and Metal Swapping. *Inorg. Chem.* **2015,** *54*, 7579-7592.
60. Clouston, L. J.; Bernales, V.; Cammarota, R. C.; Carlson, R. K.; Bill, E.; Gagliardi, L.; Lu, C. C., Heterobimetallic Complexes That Bond Vanadium to Iron, Cobalt, and Nickel. *Inorg. Chem.* **2015,** *54*, 11669-11679.
61. Enachi, A.; Baabe, D.; Zaretzke, M.-K.; Schweyen, P.; Freytag, M.; Raeder, J.; Walter, M. D., [(NHC)CoR_2]: Pre-catalysts for Homogeneous Olefin and Alkyne Hydrogenation. *Chem. Commun.* **2018,** *54*, 13798-13801.
62. Squiller, E. P.; Whittle, R. R.; Richey, H. G., Jr., Magnesiate Ions in Solutions and Solids Prepared from Dialkylmagnesium Compounds and Cryptands. *J. Am. Chem. Soc.* **1985,** *107*, 432-435.
63. Michel, O.; Meermann, C.; Törnroos, K. W.; Anwander, R., Alkaline-Earth Metal Alkylaluminate Chemistry Revisited. *Organometallics* **2009,** *28*, 4783-4790.

64. Wei, X.-H.; Coles, M. P.; Hitchcock, P. B.; Lappert, M. F., Synthesis and Structures of Five Crystalline Organometallic (Li/Y, Mg/Mg) or Coordination (Mg, Cr^{II}, Y/Y) Complexes. *Z. Anorg. Allg. Chem.* **2011,** *637*, 1807-1813.
65. Lichtenberg, C.; Jochmann, P.; Spaniol, T. P.; Okuda, J., The Allylcalcium Monocation: A Bridging Allyl Ligand with a Non-bent Coordination Geometry. *Angew. Chem. Int. Ed.* **2011,** *50*, 5753-5756.
66. Paul, S.; Morgante, P.; MacMillan, S. N.; Autschbach, J.; Lacy, D. C., Hydrogenative Catalysis with Three-Coordinate Zinc Complexes Supported with PN Ligands is Enhanced Compared to PNP Analogs. *Chem. Eur. J.* **2022,** *28*, e202201042.
67. Uzelac, M.; Hernán-Gómez, A.; Armstrong, D. R.; Kennedy, A. R.; Hevia, E., Rational Synthesis of Normal, Abnormal and Anionic NHC–gallium Alkyl Complexes: Structural, Stability and Isomerization Insights. *Chem. Sci.* **2015,** *6*, 5719-5728.
68. Mirabi, B.; Poh, W. C.; Armstrong, D.; Lough, A. J.; Fekl, U., Why Diorganyl Zinc Lewis Acidity Dramatically Increases with Narrowing C–Zn–C Bond Angle. *Inorg. Chem.* **2020,** *59*, 2621-2625.
69. This conclusion is also supported by the increase in both the deshielding of the distal CH_2 protons and the shielding of the proximal CH_2 protons in $Mo_2Cl_4(PH_2CH_2CH_2PH_2)_2$ compared to $Mo_2H_4(dpdt)_2$ (Table S5).
70. Jawiczuk, M.; Górecki, M.; Suszczyńska, A.; Karchier, M.; Jaźwiński, J.; Frelek, J., Dimolybdenum Tetracarboxylates as Auxiliary Chromophores in Chiroptical Studies of *vic*-Diols. *Inorg. Chem.* **2013,** *52*, 8250-8263.
71. Walton, R. A.; Fanwick, P. E.; Girolami, G. S.; Murillo, C. A.; Johnstone, E. V., Tetra(acetato)dimolybdenum(II). In *Inorganic Syntheses: Volume 36*, 2014; pp 78-81.
72. Anker, M. W.; Chatt, J.; Leigh, G. J.; Wedd, A. G., Preparation of Trichlorotris(tetrahydrofuran)molybdenum(III) and its Use in the Preparation of Complexes of Molybdenum(III) and -(0). *J. Chem. Soc., Dalton Trans.* **1975**, 2639-2645.
73. Neese, F., The ORCA program system. *WIREs Computational Molecular Science* **2012,** *2*, 73-78.
74. Neese, F., Software update: The ORCA program system—Version 5.0. *WIREs Computational Molecular Science* **2022,** *12*, e1606.
75. Grimme, S., Semiempirical Hybrid Density Functional with Perturbative Second-order Correlation. *J. Chem. Phys.* **2006,** *124*, 034108.
76. Johnson, E. R.; Becke, A. D., A Post-Hartree-Fock Model of Intermolecular Interactions: Inclusion of Higher-order Corrections. *J. Chem. Phys.* **2006,** *124*, 174104.
77. Lee, C.; Yang, W.; Parr, R. G., Development of the Colle-Salvetti Correlation-energy Formula into a Functional of the Electron Density. *Phys. Rev. B* **1988,** *37*, 785-789.
78. Becke, A. D., Density-functional Thermochemistry. III. The Role of Exact Exchange. *J. Chem. Phys.* **1993,** *98*, 5648-5652.
79. Andrae, D.; Häußermann, U.; Dolg, M.; Stoll, H.; Preuß, H., Energy-adjusted *ab Initio* Pseudopotentials for the Second and Third Row Transition Elements. *Theor. Chim. Acta* **1990,** *77*, 123-141.
80. Weigend, F.; Ahlrichs, R., Balanced Basis Sets of Split Valence, Triple Zeta Valence and Quadruple Zeta Valence Quality for H to Rn: Design and Assessment of Accuracy. *Phys. Chem. Chem. Phys.* **2005,** *7*, 3297-3305.

81. Staroverov, V. N.; Scuseria, G. E.; Tao, J.; Perdew, J. P., Comparative Assessment of a New Nonempirical Density Functional: Molecules and Hydrogen-bonded Complexes. *J. Chem. Phys.* **2003,** *119*, 12129-12137.
82. Weigend, F.; Furche, F.; Ahlrichs, R., Gaussian Basis Sets of Quadruple Zeta Valence Quality for Atoms H–Kr. *J. Chem. Phys.* **2003,** *119*, 12753-12762.
83. Barone, V.; Cossi, M., Quantum Calculation of Molecular Energies and Energy Gradients in Solution by a Conductor Solvent Model. *J. Phys. Chem. A* **1998,** *102*, 1995-2001.